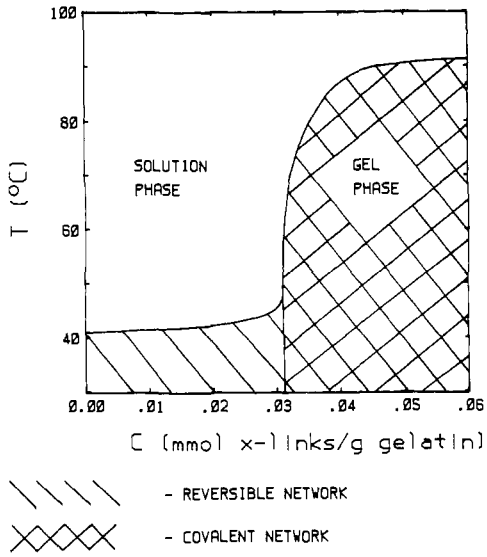

Figure 7. The phase diagram of formaldehyde cross-linked gelatin gel.

Applying this model to the gelatin system presupposes independence between the covalent and reversible cross-links. The reversible cross-links in gelatin, which result from interchain hydrogen bonds between helical regions having the nonpolar Gly-Pro-Hypro tripeptide sequence,[24] are distinct from the formaldehyde produced covalent linkages involving polar side chain lysine amino groups in the mobile amorphous regions of the polymer. That the two sets of cross-links utilize different groups on the gelatin chains suggests that a sufficient degree of independence exists to warrant application of the model. A further assumption in the approach taken here is that the increase in melting point is due solely to the covalent cross-linking. Gelatin gel does undergo an increase in melting point[32] in an annealing process.[33,34] This increase, however, is nearly completed shortly after gelation and is small relative to the very large melting point rise reported here.[35] That the T_m° obtained from extrapolation of the kinetic data is slightly higher than observed experimentally for the formaldehyde free gel may reflect some enhancement of this process in the formaldehyde-containing gels.

The close correspondence between the level of covalent cross-links resulting in the abrupt melting point rise seen in the phase diagram (Figure 7) and the critical level of covalent cross-links, C_*, determined via eq 10, supports this connectivity model. The gel region of the phase diagram, up to the critical value of 0.031 mmol of cross-links/g of gelatin, is the domain of solely the thermally reversible network. As the level of covalent cross-links increases in this domain, a decreasing fraction of the nonredundant reversible bonds is required to maintain the system as a gel and the melting point increases. The sudden increase in the thermal stability of the gel occurs with the incipient formation of the covalent network. Usually network formation is associated with a sol-to-gel transition. The formation of the covalent network here, however, takes place in the gel phase, and the network formed is in this sense a latent covalent network. The formation of this covalent network is made apparent only by the drastic change in the melting point of the system. Above the critical level of covalent cross-links the gel-to-sol transition necessarily occurs with degradation of the covalent network at what are more properly regarded as decomposition temperatures.

The melting point of a thermally reversible gel is here newly identified as a physical quantity which diverges at a critical point. Just as viscosity diverges at a critical point in solution-phase cross-linking of polymers, gel melting point diverges when the cross-linking of the polymer takes place in a thermally reversible gel phase.

Acknowledgment. The author thanks Dr. Karl J. Smith for helpful discussions.

Registry No. CH_2O, 50-00-0.

(32) Stainsby, G., In *Scientific Photography*; Sauvenier, H., Ed.; Pergamon Press: London, 1962; p 253.

(33) Djabourov, M.; Papon, P. *Polymer* **1983**, *24*, 537.
(34) Ferry, J. D. *Adv. Protein Chem.* **1948**, *4*, 20-23.
(35) The melting point of the formaldehyde free gel (Figure 3), after increasing from 33 to 36.5 °C in the interval from 30 to 450 min, increased only to 38.0 °C at 30×10^3 min.

Bond Paths and Bond Properties of Carbon–Lithium Bonds

James P. Ritchie* and Steven M. Bachrach

Contribution from the Los Alamos National Laboratory, Los Alamos, New Mexico 87545.
Received November 3, 1986

Abstract: Twenty-three organolithium compounds were analyzed by using the topological theory of molecular structure. The geometry of each compound was first optimized, making use of the 3-21G basis set. Then integrated lithium charges and quantities characterizing the carbon–lithium bond critical point, such as ρ_c(C–Li), $\nabla^2\rho_c$(C–Li), and the local energy density, were calculated. The results confirm the nature of the carbon–lithium bond to be primarily ionic. Bond path networks of these compounds were also calculated and proved surprising. Coordination numbers of lithium, as assigned by the topological theory, range from one to four. Similarly defined coordination numbers of carbon range as high as nine. Unexpectedly, some putatively bridging lithiums are not bridging in a topological sense. Additional unexpected features of the bond path networks are bond paths connecting essentially neutral carbons with lithiums and bond paths connecting highly negatively charged carbons that are widely separated. No lithium–lithium bond paths are found. Finally, unstable topological structures occur at potential energy minima. Polarization of electrons toward what are essentially lithium cations accounts for the carbon–lithium bond paths observed.

Bonds are a fundamental construct of chemistry.[1] Nevertheless, many chemists are hard pressed to define exactly what a bond is and, instead, rely upon intuition to identify bonds in unusual structures. The dotted lines that appear in representations of nonclassical cations, transition states, and "weakly" interacting systems, for example, are a sign of the uncertainty and imprecision in defining "chemical bonds".

In contrast, by a detailed examination of the behavior of the electron density distribution, the topological theory rigorously defines bonds, rings, and cages in molecules.[2] For a wide variety

(1) Pauling, L. C. *The Nature of the Chemical Bond*, 3rd ed.; Cornell University Press: Ithaca, NY, 1960.

(2) (a) Bader, R. F. W. *Acc. Chem. Res.* **1985**, *18*, 9. (b) Bader, R. F. W.; Nguyen-Dang, T. T.; Tal, Y. *Rep. Prog. Phys.* **1981**, *44*, 893.

0002-7863/87/1509-5909$01.50/0

of molecules, comparisons of results from the topological theory with those from conventional notions of bonding have shown a nearly 1:1 correspondence of the two.[3] Consequently, generally accepted, but qualitative and intuitive, chemical concepts are shown to be firmly rooted in quantum theory. Further tests and applications of the topological theory are, however, desirable.

Organolithiums have unusual geometries that challenge traditional ideas of bonding,[4] but that can be rigorously characterized from a topological analysis. While it is now recognized that the carbon–lithium bond is predominantly ionic,[4,5] the bonding in organic systems with one or more hydrogens replaced by alkali metals, which we term mixed covalent–ionic systems, has not yet been fully explained. Indeed, even the qualitative geometries of these mixed covalent–ionic systems are frequently difficult to predict. Further related questions are which atom pairs are bonded and what features of the electron density might be expected in these systems.

To answer these questions, we first performed SCF molecular orbital calculations to obtain optimized geometries and approximate wave functions for a series of organolithium compounds, most of which have been previously reported in the literature. Then the corresponding electron density distributions were characterized by using the topological theory and the results compared with classical chemical concepts.

Because the topological theory is newly developed and because we make use of only certain parts of the theory, we summarize next its relevant portions.

Summary of the Topological Theory

The topological theory defines molecular structure in terms of the electron density, ρ, and directly related quantities.[6] All these quantities are, in principle, physically observable.

Plots of ρ itself reveal few chemical features such as bonds and lone pairs; it is only when one examines how ρ changes in space that molecular structure becomes apparent. Thus the gradient vector of ρ, $\vec{\nabla}\rho$, and the Laplacian of ρ, $\nabla^2\rho$, play major roles in determining molecular structure. These quantities are defined in eq 1 and 2.

$$\vec{\nabla}\rho = (\partial/\partial x\,\hat{i} + \partial/\partial y\,\hat{j} + \partial/\partial z\,\hat{k})\rho \quad (1)$$

$$\nabla^2\rho = (\partial^2/\partial x^2 + \partial^2/\partial y^2 + \partial^2/\partial z^2)\rho \quad (2)$$

Atomic volumes are determined through the use of the vector quantity $\vec{\nabla}\rho$.[6] Paths traced out by following $\vec{\nabla}\rho$ are called gradient paths; these are paths of steepest ascent in the electron density. The space traversed by all gradient paths terminating on a single nucleus, which is a local maximum in ρ, is defined as that atom's volume or atomic basin.

These basins are quantum mechanically well-defined and individually obey the virial theorem.[6b] Properties of atoms in molecules, such as atomic charge, can therefore be calculated as an integral over an atom's basin.

Special points, called critical points, occur where $\vec{\nabla}\rho = 0$ and represent local extrema of ρ.[7] Gradient paths always originate and terminate at critical points.

Critical points are classified by their rank and signature, denoted (n, m), where n, the rank, is the number of nonzero eigenvalues of the second derivative matrix of ρ (the Hessian matrix) and m, the signature, is the number of positive eigenvalues less the number of negative ones. Critical points that are local maxima of ρ in all three orthogonal directions are $(3, -3)$ points and coincide with nuclei. Critical points that are local maxima in two directions and local minima in the third direction are $(3, -1)$ points and are called bond critical points (bond points). Two other types of critical points, ring, $(3, +1)$, and cage, $(3, +3)$, points, define rings and cages. Ring points are maxima in one direction and minima in two directions. Cage points are minima in all three directions.

Bond points are of major interest for chemists. These points lie in the common surface formed from adjacent atomic basins. They are attractors (termini) of all gradient paths that form the common surface. More importantly, bond points are the origin of two special gradient paths that initially lie along the direction of the eigenvector associated with the positive eigenvalue of the Hessian. Both of these special gradient paths will normally terminate at different nuclei. The union of these two special paths is called a bond path and it defines the line of maximum electron density between atom pairs.[8] Furthermore, the union of all bond paths in a molecule, the bond path network, describes a topological structure usually in 1:1 correspondence with chemical bond networks commonly drawn.

Stable topological structures retain the same number of critical points and the identical connectivities of these critical points with some finite geometric distortion. Unstable topological structures[9] called conflict structures,[3] while retaining the same number of critical points, yield different connectivities of the critical points wih arbitrarily small geometric distortions. It is important to note that there is no requirement of energetic stability for a topologically stable structure.[10] In fact, chemically stable structures (potential energy minima) can exhibit topologically unstable structures.

Properties of the electron density at the bond point provide information concerning the strength[3] and character[11] of the bond. For a given pair of atoms the value of ρ at the critical point, ρ_c, is a rough measure of the bond strength. In fact, Bader has shown for carbon–carbon bonds that bond length, bond strength, and ρ_c(C–C) are all interrelated.[3]

The Laplacian of ρ, $\nabla^2\rho$, indicates how concentrated or depleted the electron density is at a point relative to its neighbors.[11] Moreover, $\nabla^2\rho$ is proportional to the potential energy density plus twice the kinetic energy density. Because the potential energy density is everywhere negative and the kinetic energy density is everywhere positive, negative values of $\nabla^2\rho$ occur in regions where the potential energy is dominant. Thus, negative values of $\nabla^2\rho$ indicate regions dominated by potential energy in which electron density is locally concentrated. Positive values of $\nabla^2\rho$ indicate the local depletion of electron density.

The sign of the Laplacian at the bond point, $\nabla^2\rho_c$, is used to determine the bond type.[11] A negative value of $\nabla^2\rho_c$ indicates a dominating concentration of density along the bond path direction at the bond point, as evidenced by the negative curvature in this direction. This implies a sharing of electron density and, thus, a covalent bond. A positive value of $\nabla^2\rho_c$ shows that local depletion of electron density in the two directions perpendicular to the bond path dominates at the bond point. Ionic bonds, hydrogen bonds, and "weakly bonded" complexes all involve closed-shell interactions, resulting in positive values of $\nabla^2\rho_c$.[11]

Bonds are also characterized by the value of the local total energy density, H_c, which is equal to the sum of the potential and kinetic energy densities.[12] When $H_c < 0$, potential energy dominates, implying a concentration of charge and a covalent bond; when $H_c > 0$, kinetic energy dominates, implying a closed-shell interaction.

(3) Bader, R. F. W.; Tang, T.-H.; Tal, Y.; Biegler-Konig, F. W. *J. Am. Chem. Soc.* **1982**, *104*, 940, 946.

(4) (a) Schleyer, P. v. R. *Pure Appl. Chem.* **1983**, *55*, 355. (b) Setzner, W. N.; Schleyer, P. v. R. *Adv. Organomet. Chem.* **1985**, *24*, 354.

(5) (a) Streitwieser, A., Jr.; Williams, J. E., Jr.; Alexandratos, S.; McKelvey, J. M. *J. Am. Chem. Soc.* **1976**, *98*, 4778. (b) Klein, J.; Kost, D.; Schriver, G. W.; Streitwieser, A., Jr. *Proc. Natl. Acad. Sci. U.S.A.* **1982**, *79*, 3922. (c) Streitwieser, A., Jr. *Acc. Chem. Res.* **1984**, *17*, 353. (d) Reed, A. E.; Weinstock, R. B.; Weinhold, F. *J. Chem. Phys.* **1985**, *83*, 735.

(6) (a) Bader, R. F. W. *Acc. Chem. Res.* **1975**, *8*, 34. (b) Bader, R. F. W.; Nguyen-Dang, T. T. *Adv. Quantum Chem.* **1981**, *14*, 63.

(7) Bader, R. F. W.; Anderson, S. G.; Duke, A. J. *J. Am. Chem. Soc.* **1979**, *101*, 1389.

(8) Runtz, G. R.; Bader, R. F. W.; Messer, R. R. *Can. J. Chem.* **1977**, *55*, 3040.

(9) Bader, R. F. W.; Tal, Y.; Anderson, S. G.; Nguyen-Dang, T. T. *Isr. J. Chem.* **1980**, *19*, 8.

(10) However, see: Tal, Y.; Bader, R. F. W.; Nguyen-Dang, T. T.; Ojha, M.; Anderson, S. G. *J. Chem. Phys.* **1981**, *74*, 5162.

(11) (a) Bader, R. F. W.; Slee, T. S.; Cremer, D.; Kraka, E. *J. Am. Chem. Soc.* **1983**, *105*, 5061. (b) Cremer, D.; Kraka, E.; Slee, T. S.; Bader, R. F. W.; Lau, C. D. H.; Nguyen-Dang, T. T.; MacDougall, P. J. *J. Am. Chem. Soc.* **1983**, *105*, 5069. (c) Bader, R. F. W.; MacDougall, P. J.; Lau, C. D. H. *J. Am. Chem. Soc.* **1984**, *106*, 1594. (d) Bader, R. F. W.; Essen, H. *J. Chem. Phys.* **1984**, *80*, 1943.

(12) Cremer, D.; Kraka, E. *Croat. Chem. Acta* **1984**, *57*, 1259.

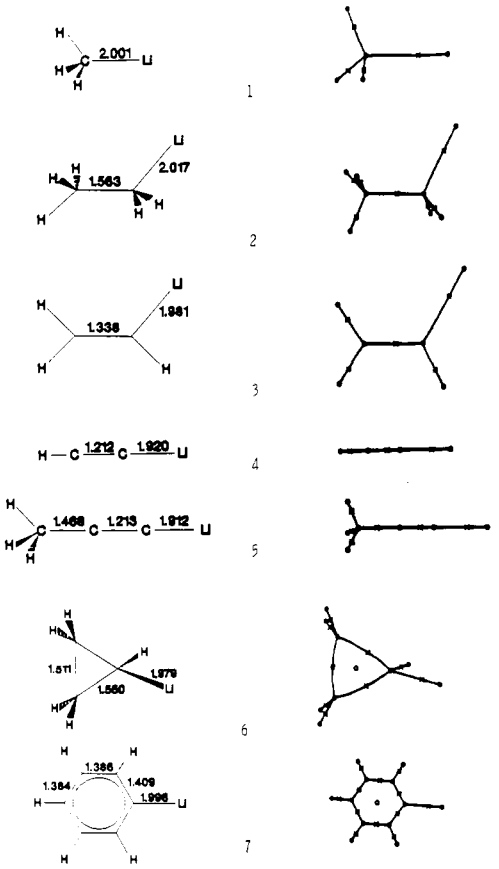

Figure 1. Geometries (left) and bond path networks (right) for simple organolithium compounds containing unicoordinate lithiums. Bond lengths are in angstroms and bond angles in degrees. Bond points are indicated with ×'s, ring points are indicated with small unfilled circles, and nuclear positions are indicated with filled circles.

Another index for characterizing bonds is the ellipticity, ϵ, defined as[11a]

$$\epsilon = \lambda_1/\lambda_2 - 1 \qquad (3)$$

In the above, λ_1 and λ_2 are the negative eigenvalues of the Hessian, with $\lambda_1 \leq \lambda_2$. A value of zero for ϵ indicates equal curvatures in the two directions orthogonal to the bond path and, thus, a perfectly cylindrical electron distribution at the bond point. Values greater than zero indicate an elliptical electron distribution at the bond point. This is typically found, for example, for double bonds; the major axis of the ellipse, that is, the softer curvature (λ_2), lies in the plane of the π bond.

Procedure

Molecular orbital calculations were performed for organolithiums mostly chosen from the literature to give a reasonable sample of lithium bonding environments. Unless otherwise noted, SCF molecular orbital calculations employing various basis sets in the original investigation characterized these structures as being of lowest energy. To simplify comparisons, we optimized the reported geometries preserving symmetry and using the 3-21G[13] basis set throughout; GAUSSIAN-82[14] was used for this purpose.

Because we are concerned with the character of the carbon–lithium bond, it is not necessary to ensure that the structures we studied are ground-state structures; this would be prohibitively expensive. It is only necessary that they be reasonable structures of relatively low energy. Put another way, given a reasonable organolithium structure, how can its bonding be discussed?

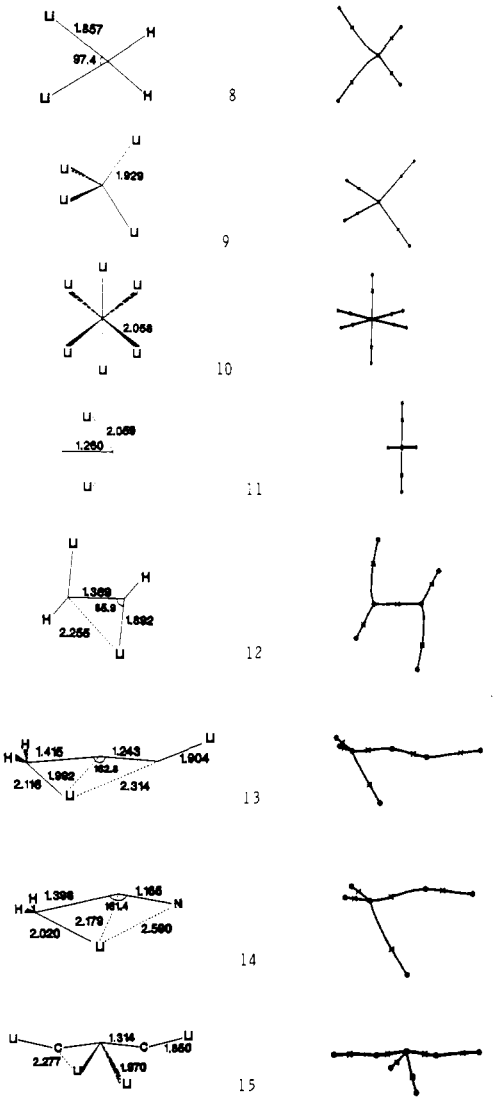

Figure 2. Geometries (left) and bond path networks (right) for other compounds containing dicoordinate lithiums. See Figure 1 caption for details.

Critical points were located and their properties calculated by using EXTREME.[15] Gradient and bond paths were generated using the RHODER[16] package. Integrations to determine the lithium charges were performed with a slightly modified version of PROAIM.[15]

Results

Coordination Numbers. Organothiums are classified according to the coordination number of the lithium obtained from the topological analysis. The coordination number[9] of an atom is taken to be equal to the number of bond paths terminating at that nucleus.

Bond paths and calculated geometries for lithium compounds found to possess unicoordinate lithiums are displayed in Figures 1 and 2. Structures **1**–**7**, shown in Figure 1, are methyllithium[5a,17] (**1**), ethyllithium[5a] (**2**), vinyllithium[18] (**3**), ethynyllithium[19] (**4**),

(13) Binkley, J. S.; Pople, J. A.; Hehre, W. J. *J. Am. Chem. Soc.* **1980**, *102*, 939.

(14) Binkley, J. S.; Frisch, M. J.; DeFrees, D. J.; Raghavachari, K.; Whiteside, R. A.; Schlegel, H. B.; Fluder, E. M.; Pople, J. A., Carnegie-Mellon University. The CTSS version was modified by Dr. R. Martin.

(15) (a) Biegler-Konig, F. W.; Nguyen-Dang, T. T.; Tal, Y.; Bader, R. F. W.; Duke, A. J. *J. Phys. B*, **1981**, *14*, 2739. (b) Biegler-Konig, F. W.; Bader, R. F. W.; Tang, T. H. *J. Comput. Chem.* **1982**, *3*, 317. The authors thank Prof. Bader for a copy of EXTREME and PROAIM.

(16) Ritchie, J. P.; Bachrach, S. M. *J. Comput. Chem.* **1987**, *8*, 499.

(17) (a) Hinchliffe, A.; Saunders, E. *J. Mol. Struct.* **1976**, *31*, 283. (b) Graham, G. D.; Marynick, D. S.; Lipscomb, W. N. *J. Am. Chem. Soc.* **1980**, *102*, 4572.

(18) Apeloig, Y.; Clark, T.; Jemmis, E. D.; Schleyer, P. v. R. *Isr. J. Chem.* **1980**, *20*, 43.

(19) (a) Veillard, A. *J. Chem. Phys.* **1968**, *48*, 2012. (b) Hinchliffe, A. *J. Mol. Struct.* **1977**, *37*, 145.

Table I. C–Li Bond Critical Point Properties[a]

	$\rho(r_c)$[b]	$\nabla^2\rho(r_c)$[c]	$H(r_c)$[d]	r_{Li}[e]	q(Li)	ϵ[f]
methyllithium (**1**)	0.042	0.230	0.0003	1.349	0.91	0.000
ethyllithium (**2**)	0.042	0.225	0.0004	1.354	0.91	0.012
vinyllithium (**3**)	0.042	0.241	0.0048	1.347	0.92	0.045
ethynyllithium (**4**)	0.042	0.270	0.0045	1.337	0.93	0.000
propynyllithium (**5**)	0.043	0.274	0.0043	1.334	0.93	0.000
cyclopropyllithium (**6**)	0.043	0.247	0.0015	1.341	0.92	0.024
phenyllithium (**7**)	0.041	0.236	0.0021	1.351	0.92	0.049
dilithiomethane (**8**)	0.041	0.297	0.0047	1.335	0.88	0.128
tetralithiomethane (**9**)	0.037	0.243	0.0034	1.368	0.86	0.000
hexalithiomethane (**10**)	0.031	0.188	0.0036	1.419	0.73	0.000
dilithioacetylene (**11**)	0.029	0.168	0.0061	1.406	0.91	1.065
	0.030[g]	0.196[g]				0.816[g]
1,2-dilithioethylene (**12**)	0.042	0.274	0.0034	1.340	0.90	0.029
1,3-dilithiopropyne (**13**)	0.042 (C_1–Li)	0.278	0.0044	1.333	0.92	0.039
	0.043 (C_1–Li)[g]	0.269[g]		1.302[g]		0.035[g]
	0.030 (C_3–Li)	0.183	0.0036	1.428	0.92[h]	0.945
	0.028 (C_3–Li)[g]	0.173[g]		1.412[g]		1.528[g]
lithioacetonitrile (**14**)	0.037	0.217	0.0023	1.377	0.92	0.118
	0.036[g]	0.200[g]		1.357[g]		0.122[g]
tetralithioallene (**15**)	0.045 (C_1–Li)	0.314	0.0045	1.315	0.89	0.005
	0.030 (C_2–Li)	0.223	0.0065	1.412	0.90	0.983
1,3-dilithiopropane (**16**)	0.030	0.192	0.0042	1.418	0.89	0.037
allyllithium (**17**)	0.033	0.206	0.0040	1.409	0.90	0.878
1,4-dilithiobutadiene (**18**)	0.029	0.178	0.0042	1.431	0.90	0.132
dilithiomethane dimer (**19**)	0.029	0.202	0.0055	1.420	0.87	0.079
	0.024	0.120	0.0018	1.492		0.128
tetralithiodiacetylide (**20**)	0.025 (Li_{eq})	0.154	0.0050	1.462	0.92	0.036
	0.023 (Li_{ax})	0.136	0.0038	1.494	0.91	0.769
methyllithium tetramer (**21**)	0.022	0.135	0.0044	1.487	0.91	0.031
1,3-dilithiocyclobutane (**22**)	0.028 (C_1–Li)	0.182	0.0039	1.446	0.89[h]	1.185
	0.028 (C_1–Li)[i]	0.163[i]		1.425[i]		1.260[i]
	0.028 (C_2–Li)	0.237	0.0074	1.423		0.204
	0.028 (C_2–Li)[i]	0.222[i]		1.395[i]		0.198[i]
dilithiocyclobutadiene (**23**)	0.028	0.213	0.0055	1.437	0.88[h]	2.368

[a] All quantities in au. Results obtained with the 3-21G Basis set, unless otherwise noted. [b] Electron density in e au^{-3}. [c] Laplacian in e au^{-5}. [d] Local energy density in hartrees au^{-3}. [e] Distance from Li to critical point in au. [f] Bond ellipticity of the carbon–lithium bond. [g] Results from calculations employing a 6-31G^{+*} basis set on carbon and a 6-31G basis on Li and H performed at the 3-21G optimized geometry. [h] These integrations took up to 30 times longer to perform than other integrations. This occurred as a result of the need to use extremely small step sizes to trace out gradient paths in these systems. Because of the numerical difficulties encountered in these cases, we believe that these quantities are not of the same precision as the other integrated charges, which are probably good to ±0.01. Our best estimate is that the resulting precision is no worse than ±0.025. [i] Results from 6-31G* calculations performed at the 6-31G* optimized geometry.

propynyllithium[20] (**5**), cyclopropyllithium[21,22] (**6**), and phenyllithium[23] (**7**). These are simple monolithio hydrocarbons expected to provide straightforward analysis and reliable benchmarks. Structures shown in Figure 2 are dilithiomethane[21,24] (**8**), tetralithiomethane[21,25] (**9**), hexalithiomethane[26] (**10**), dilithioacetylene[27] (**11**), 1,2-dilithioethylene[18,28] (**12**), 1,3-dilithiopropyne[20] (**13**), lithioacetonitrile[29] (**14**), and tetralithioallene[20] (**15**).

Compounds containing dicoordinate lithium are shown in Figure 3: 1,3-dilithiopropane[30] (**16**), allyllithium[31] (**17**), 1,4-dilithio-

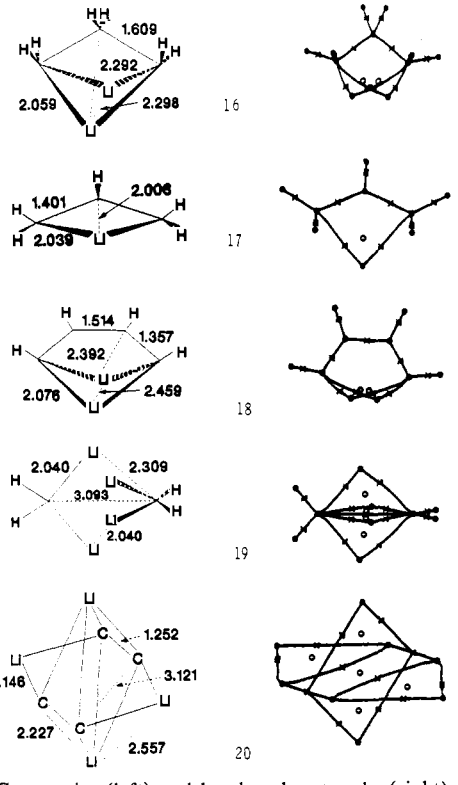

Figure 3. Geometries (left) and bond path networks (right) for compounds containing dicoordinate lithiums. See Figure 1 caption for details.

(20) Jemmis, E. D.; Chrandarsekhar, J.; Schleyer, P. v. *R. J. Am. Chem. Soc.* **1979**, *101*, 2848.
(21) Collins, J. B.; Dill, J. D.; Jemmis, E. D.; Apeloig, Y.; Schleyer, P. v. R.; Seeger, R.; Pople, J. A. *J. Am. Chem. Soc.* **1976**, *98*, 5419.
(22) Skancke, A.; Boggs, J. E. *J. Mol. Struct.* **1978**, *50*, 173.
(23) Greenberg, A.; Liebman, J. F. *Tetrahedron* **1979**, *35*, 2623.
(24) (a) Laidig, W. D.; Schaefer, H. F., III. *J. Am. Chem. Soc.* **1978**, *100*, 5972. (b) Bachrach, S. M.; Streitwieser, A., Jr. *J. Am. Chem. Soc.* **1984**, *106*, 5818.
(25) Wurthwein, E. U.; Sen, K. D.; Pople, J. A.; Schleyer, P. v. R. *Inorg. Chem.* **1983**, *22*, 496.
(26) (a) Schleyer, P. v. R.; Wurthwein, E. U.; Kaufmann, E.; Clark, T.; Pople, J. A. *J. Am. Chem. Soc.* **1983**, *105*, 5930. (b) Reed, A. E.; Weinhold, F. *J. Am. Chem. Soc.* **1985**, *107*, 1919.
(27) (a) Apeloig, Y.; Schleyer, P. v. R.; Binkley, J. S.; Pople, J. A.; Jorgenson, W. L. *Tetrahedron Lett.* **1976**, 3923. (b) Ritchie, J. P. *Tetrahedron Lett.* **1982**, *23*, 4999.
(28) Schleyer, P. v. R.; Kaufmann, E.; Kos, A. J.; Clark, T.; Pople, J. A. *Angew. Chem., Int. Ed. Engl.* **1986**, *25*, 169.
(29) (a) Moffat, J. G. *J. Chem. Soc., Chem. Commun.* **1980**, 1108. (b) Kaneti, J.; Schleyer, P. v. R.; Clark, T.; Kos, A. J.; Spitznagel, G. W.; Andrade, J. G.; Moffat, J. D. *J. Am. Chem. Soc* **1986**, *108*, 1481.
(30) Schleyer, P. v. R.; Kos, A. J.; Kaufmann, E. *J. Am. Chem. Soc.* **1983**, *105*, 7617.
(31) Clark, T.; Rohde, C.; Schleyer, P. v. R. *Organometallics* **1983**, *2*, 1344.

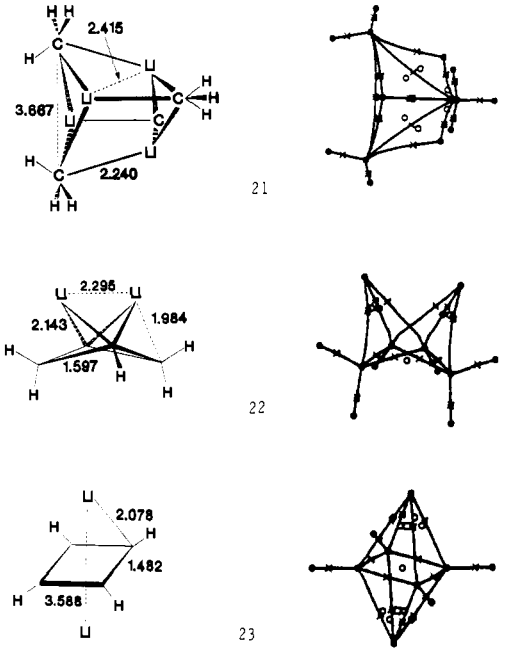

Figure 4. Geometries (left) and bond path networks (right) for compounds containing tri- and tetracoordinate lithiums. Cage points are denoted with a square. For clarity, the bond paths of **21** are shown for a projection into a symmetry plane. See Figure 1 caption for further details.

1,3-butadiene[32] (**18**), dilithiomethane dimer[33] (**19**), and tetralithiodiacetylide[34] (**20**).

Examples of tricoordinate and tetracoordinate lithium are shown in Figure 4: methyllithium tetramer[35] (**21**), 1,3-dilithiocyclobutane[36] (**22**), and dilithiocyclobutadiene[32] (**23**).

Bond Point Properties. Table I shows values of ρ_c(C–Li), $\nabla^2\rho_c$(C–Li), H_c(C–Li), integrated lithium net charge, and distance from the carbon–lithium bond point to lithium for the 23 compounds shown in Figures 1–4. Unless otherwise noted, results were obtained with the 3-21G basis.

Values of ρ_c(C–Li) range from 0.022 to 0.045 e au^{-3}. Simple monolithio hydrocarbons, **1–7**, show values insensitive to the hybridization of carbon in the narrow range from 0.041 to 0.043 e au^{-3}. Other compounds with values lying within or near this range are dilithiomethane (**8**, 0.041), 1,2-dilithioethylene (**12**, 0.042), the C_1–Li bond in 1,3-dilithiopropyne (**13**, 0.042), and the C_1–Li bond in tetralithioallene (**15**, 0.045). Otherwise, values range from 0.022 to 0.037 e au^{-3}.

Typical values of ρ_c(C–C) obtained with the 3-21G basis set are as follows: ethane, 0.218; ethylene, 0.339; acetylene, 0.408 e au^{-3}. Prototypical ionic bonds give the following ρ_c: LiF, 0.089; NaF, 0.067; LiCl, 0.032; NaCl, 0.026 e au^{-3}.

Values of $\nabla^2\rho_c$(C–Li) and H_c(C–Li) are positive for all compounds examined.[12,37] The range of $\nabla^2\rho_c$(C–Li) is 0.120–0.314 e au^{-5}. Values of $\nabla^2\rho_c$ for prototypical ionic bonds with the 3-21G basis set are as follows: LiF, 0.727; NaF, 0.589; LiCl, 0.233; NaCl, 0.216 e au^{-5}. Simple organolithiums **1–7** have values of $\nabla^2\rho_c$(C–Li) ranging between 0.225 and 0.270 e au^{-3} that increase roughly with hybridization of carbon as $sp^3 < sp^2 < sp$. Results for the other molecules show this correlation not to be general.

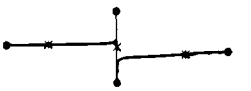

Figure 5. Bond path network of dilithioacetylene in which the lithiums have been rotated unsymetrically toward opposite carbons.

Also listed in Table I are distances, r_{Li}, from lithium to the C–Li bond critical point. Values of r_{Li} range from 1.333 to 1.494 bohr (0.71–0.79 Å). A much narrower range is obtained for the simple organolithiums **1–7**. Interestingly, crystallographic studies of minerals give an ionic radius of hexacoordinate lithium of 0.76 Å,[38] which is within the range calculated. We did not find r_{Li} to increase with coordination number as is generally assumed to occur.

Integrated lithium charges of around 0.90, shown in Table I, are direct calculational evidence of the large degree of charge -transfer that has occurred from lithium to carbon. Its range is rather small, except for hexalithiomethane (**10**).

Bond ellipticities are also listed in Table I. The values are generally small, indicating a nearly cylindrical electron distribution at the bond point. Exceptions are noted, however, when lithium is near to and oriented with a π system, as in **11**, **13**, **17**, **20**, and **23**. Additionally, **22**, which possess a lithium poised between two orbitals with substantial amounts of ρ character, has a large value of the bond ellipticity. In these cases, the major axis of curvature is in the direction of the π system.

Small values of ρ_c(C–Li), positive values of $\nabla^2\rho_c$(C–Li), values of r_{Li} similar to those obtained from crystal structures of minerals, and integrated lithium charges near 0.9 accord with the concept of a predominantly ionic carbon–lithium bond.[5] Relatively small ranges were also noted for these calculated quantities, indicating a very similar carbon–lithium interaction in all cases. Thus the compounds studied here are all shown to have predominantly ionic carbon–lithium bonds.

Bond Path Networks Having Unicoordinate Lithiums. Figures 1 and 2 show bond path networks of compounds with unicoordinate lithiums. For convenience and comparison geometrical structures are drawn on the left to indicate pertinent internuclear separations.

The simple organolithiums **1–7** show the expected bond paths. Likewise, polylithiomethanes **8–10** show simple bond paths, thus excluding any bonding models with significant Li–Li bonding. Structure **8**, which contains a planar carbon atom, is not the global minimum on the potential energy surface; however, it is a local minimum. The tetrahedral structure of dilithiomethane is favored by 10 kcal mol^{-1} over the planar form at the 4-31G level.[21]

Dilithioacetylene, **11**, is an example of an unstable topological structure that is a potential energy minimum, although the linear isomer is slightly lower in energy at 4-31G.[27,34] The bond path network of **11**, shown in Figure 2, has bond paths connecting the lithiums with the carbon–carbon bond point. Normally, bond paths connect atoms to atoms. In **11**, however, one of the gradient paths originating from each carbon–lithium bond point terminates at the carbon–carbon bond point. Stepping toward lithium from the carbon–carbon bond point leads to an initial decrease in electron density; farther along this path, the density begins to increase as the lithium atom is encountered. The point of minimum density along this path is the carbon–lithium bond point. C_2Be and π complexes have been found to possess this same topological structure.[39]

Arbitrarily small displacements of the lithiums, however, result in different topological structures. Figure 5 shows the bond path network obtained when the lithiums are both rotated slightly toward opposite carbons. The bond paths now connect each lithium with a single carbon, although they just miss the carbon–carbon bond point. This geometric distortion results in a rise of the calculated energy and, indeed, it is known that **11** is a minimum in the potential energy surface at 4-31G, which should

(32) Kos, A. J.; Schleyer, P. v. R. *J. Am. Chem. Soc.* **1980**, *102*, 7929.
(33) Jemmis, E. D.; Schleyer, P. v. R.; Pople, J. A. *J. Organomet. Chem.* **1978**, *154*, 327.
(34) Disch, R. L.; Schulman, J. M.; Ritchie, J. P. *J. Am. Chem. Soc.* **1984**, *106*, 6246.
(35) (a) Guest, M. F.; Hillier, I. H.; Saunders, V. R. *J. Organomet. Chem.* **1972**, *44*, 59. (b) Graham, G.; Richtsmeier, S.; Dixon, D. A. *J. Am. Chem. Soc.* **1980**, *102*, 5759. (c) Clark, T.; Schleyer, P. v. R.; Pople, J. A. *J. Chem. Soc., Chem. Commun.* **1978**, 137.
(36) Bachrach, S. M. *J. Am. Chem. Soc.* **1986**, *108*, 6406.
(37) Bader, R. F. W.; MacDougall, P. J. *J. Am. Chem. Soc.* **1985**, *107*, 6788.
(38) (a) Shannon, R. D.; Prewitt, C. T. *Acta Crystallogr., Sect. A* **1969**, *25*, 925. (b) Shannon, R. D. *Acta Crystallogr., Sect. A* **1976**, *32*, 751.
(39) (a) Cremer, D.; Kraka, E. *J. Am. Chem. Soc.* **1985**, *107*, 3800. (b) Koch, W.; Frenking, G.; Gauss, J.; Cremer, D.; Sawaryn, A.; Schleyer, P. v. R. *J. Am. Chem. Soc.* **1986**, *108*, 5732.

be analogous to the 3-21G results.[26] Consequently, a topologically unstable structure is shown to correspond with an energetically stable structure.

Molecules **12–15** contain putatively bridging lithiums based on geometrical considerations that are unicoordinate by topological criteria. There are several indications that these putatively bridging lithiums do indeed have significant interactions with more than one atom. The pronounced bending of the heavy atom skeleton toward the putatively bridging lithiums is one. Multiple and short carbon–lithium separations is another. Electrostatic arguments also suggest that the putatively bridging lithiums should have significant interactions with the terminal anionic atoms of **12–15**. Despite this, the lithiums are the end points of only one bond path.

Structure **12** is not the global minimum on the dilithioethylene surface at 3-21G, in contrast to higher level calculations.[28] Nevertheless, **12** is at least a local minimum for all levels of theory. The position of the lithium atoms as putatively bridging has been argued in terms of a syn-hydrogen–lithium attraction.[18] However, we find no bond path between these atoms.

Bond Path Networks Having Dicoordinate Lithiums. Structures **16–20**, shown in Figure 3, possess topologically bridging lithiums that are dicoordinate.

Structure **19** is notable for several reasons. Each lithium is connected to both carbons, even though the carbon–lithium distances differ significantly: 2.040 and 2.309 Å. It is also found that each carbon and the nearer lithiums lie in the same plane as the hydrogens on the carbon. As has been previously noted, **19** thus contains planar carbons.[33] Finally, the carbons are connected by a bond path, despite a large internuclear separation of 3.093 Å.

The bond path network for **20** possesses twelve bond and five ring points. Furthermore, although the equatorial lithiums are connected to carbons via usual bond paths, both axial lithiums are linked to two carbon–carbon bond points in a manner resembling that found in dilithioacetylene, **11**. This structure is, therefore, topologically unstable with regard to small movements of the axial lithiums, even though **20** represents an energy minimum at 4-31G, which presumably mimics the 3-21G calculation.[34]

The number of rings and their constituent atoms are another point of interest in **20**. Bond paths are found to link the carbons of different acetylide units, notwithstanding an internuclear separation of 3.121 Å. Consequently, a four-membered carbon ring is found along with two C–C–Li three-membered rings. Two more ring points are found above and below the carbon plane. The rings that they define illustrate the unusual feature of having one side, which they share, that is not a bond path and two sides that are bond paths connecting atoms to a bond critical point.[40]

Bond Path Networks Having Tri- or Tetracoordinate Lithium. Figure 4 shows examples of tricoordinate lithium and a tetracoordinate lithium.

The geometry of methyllithium tetramer, **21**, symmetry group T_d, is in reasonable accord with the known crystal structure.[41] Its bond path network features tricoordinate lithiums. Bond paths are also observed between carbons, despite a separation of 3.667 Å. Altogether, **21** has twelve carbon–lithium bond paths and six carbon–carbon bond paths, resulting in twelve C–C–Li three-sided rings and a single cage point. Twelve carbon–hydrogen bond paths are also present.

Structure **22**, 1,3-dilithiocyclobutane, has been reported previously.[36] Of interest here is the bond path connecting a methylenic carbon to lithium, in addition to the bond paths connecting lithium to the anionic carbons. As a result, **22** possesses five rings.

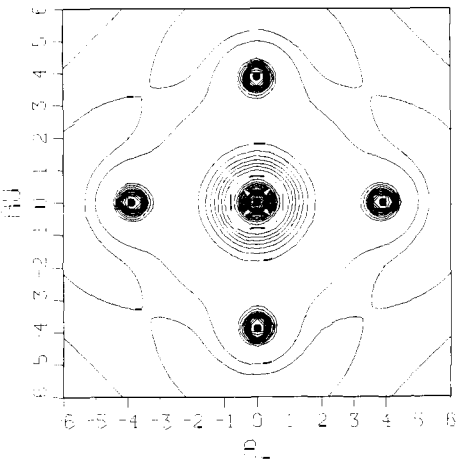

Figure 6. ρ for the HOMO of CLi_6 (**10**). Contours range from 5×10^{-4} to 5×10^{-3} in increments of 5×10^{-4} e au^{-3}.

Structure **23** is shown to be a cyclobutadieneyl dianion with capping lithiums, as previously suggested.[32] Bond paths connect both lithiums with all four carbons, giving rise to cage points, denoted by the squares in **23**, above and below the four-membered ring. Ring points result from the eight C–C–Li rings and the single-carbon four-membered ring.

Influence of Basis Set Size. The geometry of 1,3-dilithiocyclobutane, **22**, was reoptimized and bond paths recalculated by using the 6-31G*[42] basis set. This basis set includes d orbitals on both carbon and lithium.

The resulting bond path network is indistinguishable from that shown in Figure 4. Values of bond point properties, shown in Table I, do not differ in a significant way from those obtained with the 3-21G basis set.

Single-point calculations for dilithioacetylene (**11**), 1,3-dilithiopropyne (**13**), and lithioacetonitrile (**14**) were performed at the 3-21G optimized geometry employing a 6-31G basis set that was supplemented by d and diffuse[43] sp shells on carbon, to account properly for its anionic character.

The resulting topological structures are indistinguishable from those shown in Figure 2. Values of bond point properties for the carbon–lithium bond, shown in Table I, do not differ in a significant way from those obtained with the 3-21G basis set.

Finally, previous topological studies have been performed on methyllithium (**1**). Using the 6-31G** basis set, Bader[37] reports values of $q(\mathrm{Li}) = +0.90$ e and $\rho_c(\mathrm{C–Li}) = 0.042$ e au^{-3}. Cremer,[12] using the 6-31G* basis set, finds the values of $\rho_c(\mathrm{C–Li}) = 0.042$ e au^{-3} and $\nabla^2\rho_c(\mathrm{C–Li}) = 0.204$ e au^{-5}. These results are very similar to the values at 3-21G shown in Table I.

The above results show that calculated quantities in Table I and bond paths obtained with the 3-21G basis are not seriously in error.

Discussion

Results of the topological analysis shown in Table I confirm the ionic character of the carbon–lithium bond.[5]

Unlike the bond point properties of covalent bonds,[11a] those of ionic bonds vary only slightly and are found to be relatively insensitive to environment. Our results show that with the exception of hexalithiomethane, values of the charge on lithium, $\rho_c(\mathrm{C–Li})$, and $\nabla^2\rho_c(\mathrm{C–Li})$ are small and nearly constant, regardless of bonding environment and coordination number.

Values shown in Table I for hexalithiomethane do not indicate a qualitatively different situation. In hexalithiomethane, which represents an extreme bonding environment, only the charge on

(40) The sides of a ring can be located in a straightforward manner. The ring critical point will be the origin of a number of gradient paths that terminate at other critical points. These terminal critical points can be any type of critical that can be a terminus, be it a nucleus, bond, or ring point. There will be twice as many terminal critical points as sides in the ring. Usually, half of these terminal points are nuclei and half are bond points. The sides of the ring are then bond paths. In **20**, however, two of the three-sided rings share a side that connects a ring point with bond points on either side (not drawn in the figure). The other two sides are formed of a bond path that links lithium to the carbon–carbon bond point.

(41) (a) Weiss, E.; Lucken, E. A. C. *J. Organomet. Chem.* **1964**, *2*, 197. (b) Weiss, E.; Hencken, G. *J. Organomet. Chem.* **1970**, *21*, 265.

(42) (a) Hehre, W. J.; Ditchfield, R.; Pople, J. A. *J. Chem. Phys.* **1972**, *56*, 2257. (b) Harihan, P. C.; Pople, J. A. *Theor. Chim. Acta* **1973**, *28*, 213.

(43) Clark, T.; Chandrasekhar, J.; Spitznagel, G. W.; Schleyer, P. v. R. *J. Comput. Chem.* **1983**, *4*, 294.

lithium differs noticeably from that found for other, more usual, organolithiums. This difference likely arises from a saturation of the charge-bearing ability of carbon or, in other words, an excess of electrons over valence orbitals on carbon, rather than any fundamental difference in the carbon–lithium bond. Nevertheless, the carbon atom is assigned a charge of −4.38. This result contrasts with a charge of −3.44 determined by natural population analysis[26b] and −0.93 determined from Mulliken analysis.[26a] Examination of ρ for the HOMO of CLi_6, shown in Figure 6, reveals essentially no LiLi bonding density and describes, instead, localized density on lithium and, to a lesser extent, carbon. Evidently, partial occupation of the 3s-like orbital is energetically feasible due to electrostatic stabilization from the six lithium cations. Indeed, models using the integrated charges suggest that hexalithiomethane is an excellent example of the electrostatic stabilization of a highly charged species by association with oppositely charged ions.

Interestingly, when more than one lithium is present in an organolithium, the lithium–lithium separation is frequently less than that found in diatomic lithium. So, while 2.672 Å is the observed[44] separation in Li_2 (2.816 Å is calculated at 3-21G[13]), Li–Li separations shorter than this are commonly found for the organolithiums shown in Figures 3 and 4; yet, no Li–Li bond paths result. The anionic moiety in organolithiums holds lithium cations closer together than do the two valence electrons of Li_2.

Ionic bonds also result in unique and surprising features of the electron density that are revealed by the topological structures. Bond paths for covalent bonds are usually in 1:1 correspondence with expectations based upon traditional notions of bonding. On the other hand, bond path networks for organolithiums, and we suspect polyatomic mixed covalent–ionic systems in general, may be quite unexpected.

We emphasize that bond path networks provide direct information about the calculated electron density distribution. Each bond path is the line between two atoms along which the electron density is a maximum.[39a] As such, their unexpected nature is evidence of a fundamental lack of understanding about how electrons are distributed in these systems.

A simple approach to drawing bonds in ionic systems might coordinate cations to atoms within "reasonable" distances that bear charge in important resonance structures of the isolated anion. This approach certainly picks out energetically important pairwise contributions; it also yields structures in agreement with the calculated topological structure for **1–10**, **16–18**, and **23**. On the other hand, it does not explain the topologically unstable structures **11** and **20**, the absence of expected bond paths connecting lithium to charge-bearing atoms in structures **12–15**, and the presence of unexpected bond paths connecting lithium to non-charge-bearing carbons in structure **22**. In addition, this simple model fails to account for the presence of bond paths between distant and similarly charged carbons in structures **19**, **20**, and **21**.

We propose that the most important effect governing the appearance of carbon–lithium bond paths is polarization.

Polarization has been previously recognized as an important effect in ionic bonding. Bader[45] showed that, compared with the superposition of isolated spherical ions, the flouride ion in LiF is polarized to add density to the internuclear region and the cation is polarized to remove electron density from the internuclear region. This polarization, Bader points out, can be viewed as a requirement of the Hellmann–Feynman theorem: spherical anions place too little electron density in the internuclear region, where electron density leads to binding forces, to balance the force of cation–anionic nucleus repulsion; spherical cations experience an attractive force resulting from the anion and so back-polarize to balance it. We also note that, in addition to the dominant forward-polarization of the anion, significant amounts of back-polarization are also observed.

Thus, study of simple ionic systems shows that electrostatic forces result in polarization of charge toward the cation.[37,45] In simple diatomic ions, such as LiF, bond paths occur between ions as a result of symmetry, regardless of polarization effects. Nevertheless, in polyatomic systems, we expect that sufficient polarization of electron density toward a cation will result in a bond path.

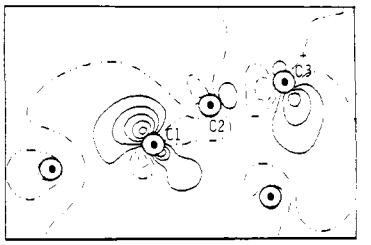

Figure 7. Plot of 1,3-dilithiopropyne molecular electron density less that of the isolated ions. The electron density of the isolated anion was obtained with the lithium basis functions present where the lithium nuclei are in the neutral. This was done to account at least partially for the basis set superposition error. Solid contours indicate positive values, dashed contours indicate negative values, and the dot–dot–dash contour indicates zero as a value. Contour increment is constant at 0.01 e au^{-3} (=0.067 e $Å^{-3}$). Positions of atoms in the plane are shown with heavy filled-in circles and regions close to these nuclei are blanked out for clarity of presentation. The projected positions of the two hydrogens not in the plane are indicated by the plus sign.

In the organolithiums studied in this work, polarization effects account for all the carbon–lithium bond paths illustrated in the figures.

For systems in which a single atom carrying a nearly unit negative charge interacts with the single available lithium, this model yields simple bond paths in agreement with those found for **1–7** and for the terminal C–Li bonds in tetralithioallene (**15**). Carbons carrying multiple negative charges are especilly polarizable and can coordinate with all lithiums within a reasonable distance, as evidenced in the polylithiomethanes (**8**, **9**, and **10**) and dilithiomethane dimer (**19**).

1,2-Dilithioethylene (**12**), 1,3-dilithiopropyne (**13**), lithioacetonitrile (**14**), and tetralithioallene (**15**) show ample structural evidence of having multiple lithium–anionic carbon interactions and yet the lithiums are all topologically unicoordinate. We suggest that these systems be viewed as composed of primary anionic carbon–lithium and secondary anionic carbon–lithium interactions, the primary interactions being those associated with the shortest separation. Primary interactions result in bond paths, while other interactions do not. Apparently, the lithium sufficiently "hardens" its anionic carbon partner in a primary carbon–lithium interaction such that polarization of the anionic carbon toward more distant lithiums is too weak to result in a bond path.

A map of the 1,3-dilithiopropyne molecular electron distribution less that resulting from a superposition of the dianion and two lithium cations illustrates this effect. The map, shown in Figure 7, clearly shows strong polarizations arising from the primary anionic carbon–lithium interactions that result in bond paths; these bond paths are not, however, precisely along the direction of strongest polarization. A weak polarization toward the putatively bridging lithium is found on C_1, but does not yield a bond path.

In cases where no distinction is possible between primary and secondary anionic carbon–lithium interactions, topologically bridging lithiums occur. Thus, the lithiums of 1,3-dilithiopropane (**16**), allyllithium (**17**), 1,4-dilithiobutadiene (**19**), methyllithium tetramer (**21**), 1,3-dilithiocyclobutane (**22**), and dilithiocyclobutadiene (**23**) are connected via bond paths with more than one symmetry-equivalent carbon. A similar situation occurs for the equatorial lithiums of tetralithiodiacetylide (**20**).

The unstable topological features found in **11** and **20** result, in our view, from the especially large polarizability of the acetylide fragment and its (American) football-like shaped charge distribution.

(44) Herzberg, G. *Spectra of Diatomic Molecules*; Van Nostrand Reinhold: Princeton, NJ, 1970.

(45) (a) Bader, R. F. W.; Henneker, W. H. *J. Am. Chem. Soc.* **1965**, *87*, 3063. (b) Bader, R. F. W. In *The Force Concept in Chemistry*; Deb, B. M., Ed.; Van Nostrand Reinhold: New York, 1981; p 39.

The existence of neutral carbon–lithium bond paths, such as those found in 1,3-dilithiocyclobutane (**22**), are explained as the polarization of the methylenic carbon's electrons toward lithium. This system is unique in that a reasonably polarizable neutral carbon is in proximity to a lithium cation. In classical terms, this "bond" might be described as dative. Other systems possess either too large a carbon–lithium separation or an inadequately polarizable carbon to yield this type of carbon–lithium bond path.

Polarizability also plays a central role in accounting for the hypercoordination of carbon in ionic compounds. Structures **16**, **22**, and **23** have pentacoordinate carbon; structure **10** exhibits hexacoordinate carbon; **19** has heptacoordinate carbon; and **21** features nonacoordinate carbons. The last two examples include unusual carbon–carbon bond paths. Carbon–lithium coordination arises from polarization of electron density on carbon toward the cation. There is little or no sharing of electron density, as indicated by the small values of ρ_c(C–Li) and positive values of $\nabla^2\rho_c$(C–Li). Similar behavior is observed at the C–C bond points. Thus the observed hypercoordination is not hypervalency, which requires a sharing of electron pairs.[46]

The carbon–carbon bond paths of the widely separated hypercoordinated carbons in **19**, **20**, and **21** occur between atoms that traditional theory would regard as repelling one another. These bond paths link highly negatively charged carbons separated by 3.093 Å in dilithiomethane dimer (**19**), 3.121 Å in tetralithiodiacetylide (**20**), and 3.667 Å in methyllithium tetramer (**21**). Thus, electrostatic repulsion is expected to dominate the interaction between these connected carbons because, in the limit of complete ionic character, there are no partially filled orbitals available for covalent bonding.

We, however, find that there are indeed some attractive forces that operate between these connected carbons. The total Hellmann–Feynman force between the two connected carbons is attractive, the Hellmann–Feynman force of the electrons of one carbon on the other nucleus is attractive, and the Hellmann–Feynman self-force is likewise attractive. Furthermore, complete electron transfer from lithium to carbon does not occur, leaving partially filled bonding orbitals. It is unlikely that operation of these forces results in a net attraction between these widely separated but connected atoms. Nevertheless, they may result in a force between the atoms less repulsive than it otherwise would be. In any case, the topology of the charge distribution between these widely separated, highly charged carbons is identical with that found between carbons in ethane, for example. We are thus driven to conclude that bond paths do not correspond with traditional chemical thinking in all cases, but they may be indicating the existence of some attractive force between the connected atoms. What is needed is a method whereby the total quantum mechanical forces operating between two basins can be calculated, but this is not our purpose here.

(46) Lewis, G. N. *Valence and the Structure of Atoms and Molecules*; Chemical Catalog Co.: New York, 1926.

Conclusions

Organolithiums of a wide variety were confirmed to possess predominantly ionic carbon–lithium bonds. They also have normal covalent carbon–carbon and other bonds. consequently, we term them mixed covalent–ionic systems.

Mixed covalent–ionic systems, such as the organolithiums examined in this work, exhibit surprising bond path networks. Polarization effects explain the presence or absence of carbon–lithium bond paths. Bond paths between widely separated and highly negatively charged carbons, however, are not easily explained.

Polarization of electron density toward a cation is the prime cause of the carbon–lithium bond paths observed. We also find that a strong carbon–lithium interaction can "harden" the carbon, preventing coordination with more distant lithiums. Also, polarizable but essentially neutral carbons can be connected to lithium via a bond path.

No Li–Li bond paths were observed and, hence, Li–Li bonding in these compounds plays only a minor role, if any, in determining their structures and energies.

Acknowledgment. This work was conducted under the auspices of the U.S. Department of Energy. S.M.B. acknowledges the support of the Director's Postdoctoral program.